nature structural & molecular biology

Defining the structural relationship between kainate-receptor deactivation and desensitization

G Brent Dawe[1,2,4], Maria Musgaard[3,4], Elizabeth D Andrews[2], Bryan A Daniels[2], Mark R P Aurousseau[2], Philip C Biggin[3,4] & Derek Bowie[2,4]

Desensitization is an important mechanism curtailing the activity of ligand-gated ion channels (LGICs). Although the structural basis of desensitization is not fully resolved, it is thought to be governed by physicochemical properties of bound ligands. Here, we show the importance of an allosteric cation-binding pocket in controlling transitions between activated and desensitized states of rat kainate-type (KAR) ionotropic glutamate receptors (iGluRs). Tethering a positive charge to this pocket sustains KAR activation, preventing desensitization, whereas mutations that disrupt cation binding eliminate channel gating. These different outcomes explain the structural distinction between deactivation and desensitization. Deactivation occurs when the ligand unbinds before the cation, whereas desensitization proceeds if a ligand is bound without cation pocket occupancy. This sequence of events is absent from AMPA-type iGluRs; thus, cations are identified as gatekeepers of KAR gating, a role unique among even closely related LGICs.

Structural and functional biologists have long sought to understand the mechanisms by which LGICs respond to small chemical ligands and modulators. Seminal work established the general principle that LGICs not only are activated by biologically derived molecules, such as the neurotransmitter acetylcholine[1], but also are inactivated by prolonged exposure to these molecules through a process universally known as desensitization[2]. Since this work, almost all LGICs have been shown to desensitize. For example, desensitization is thought to shape signaling within the vertebrate central nervous system by affecting the fast chemical transmission mediated by iGluRs along with $GABA_A$ and glycine receptors[3]. From all of this work, it has been concluded that the conformational events that lead to the occurrence of deactivation and the onset of desensitization are governed by the physicochemical properties of the bound ligand[4]. In support of this, pioneering work on native AMPA-type iGluRs (AMPARs) has shown that even modest changes to the ligand structure have profound effects on the rates and degree of desensitization[5].

During the last decade, structural and functional analyses of LGICs have revealed that the molecular basis of channel gating may be quite distinct for different ion-channel families[6–8]. For the iGluR family, numerous mechanistic details of activation and desensitization have been identified and extensively commented upon[9–11]. After the elucidation of the ligand-binding domain (LBD) structure[12], a mechanism of iGluR desensitization was proposed, involving the separation of subunits that are assembled as dimers at the LBD[13]. This mechanism has been supported by additional crystal structures that captured AMPARs in different functional states[14]. Accordingly, efforts to engineer iGluR receptors that lack desensitization have focused on constraining movement at the LBD dimer interface. From this, covalent cross-linking of the dimer interface has been shown to generate AMPARs and KARs that yield nondecaying currents upon sustained agonist application[15,16]. Similar experiments on NMDA-type iGluRs have offered a more nuanced explanation of LBD function by uncovering the structural[17] and single-channel effects[18] of dimer cross-linking. Specifically, they propose that constriction of the dimer interface primarily affects open-channel probability and not desensitization[18]. This observation suggests that a more in-depth single-channel analysis of the mechanism of AMPAR and KAR desensitization is warranted.

Here, we set out to study the molecular basis of KAR desensitization by evaluating mutants that are proposed to block it[15,19]. In both cases, the mutations are located in the GluK2 KAR LBD dimer interface, which not only is implicated in receptor desensitization but also contains binding pockets for both sodium and chloride ions[20,21]. Prior work from our laboratory shows that external ions are an absolute requirement for GluK2 receptor activation[22], yet their precise role in desensitization is unresolved[21,23]. Our present data identify that desensitization of KARs proceeds only if a ligand is bound without cation pocket occupancy, whereas deactivation occurs when the ligand unbinds before the cation. This sequence of events identifies external cations as pivotal in directing KARs into active states or long-lived desensitized states.

RESULTS

KARs desensitize with or without prior channel activation

To observe the microscopic behavior of KAR desensitization, we excised outside-out patches from transfected mammalian cells

[1]Integrated Program in Neuroscience, McGill University, Montréal, Québec, Canada. [2]Department of Pharmacology and Therapeutics, McGill University, Montréal, Québec, Canada. [3]Department of Biochemistry, University of Oxford, Oxford, UK. [4]These authors contributed equally to this work. Correspondence should be addressed to P.C.B. (philip.biggin@bioch.ox.ac.uk) or D.B. (derek.bowie@mcgill.ca).

Received 19 March; accepted 17 July; published online 18 August 2013; doi:10.1038/nsmb.2654

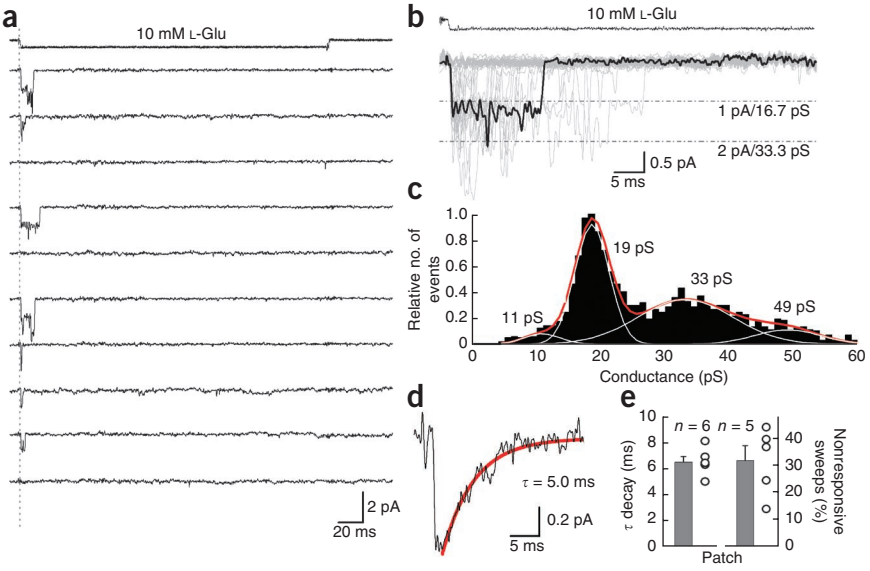

Figure 1 Kainate-receptor desensitization occurs with or without channel activation. (**a**) Typical GluK2 receptor unitary current events elicited by 10 mM L-glutamate (L-Glu; 250-ms pulse duration) in an outside-out patch recording (patch no. 12212p1, –60 mV). (**b**) Overlay of 45 individual current records from the same patch shown in **a**. A typical opening elicited by L-glutamate is shown in thick line. (**c**) GluK2 conductance distributions plotted after time-course fitting. (**d**) Averaged individual current records from the patch in **a** and **b**, showing an ensemble response with a decay fit by a single exponential function whose time constant, τ, is shown. (**e**) Left, decay time constants of ensemble responses from several patches. Right, fraction of L-glutamate applications that did not elicit a measureable response from receptors. Error bars, s.e.m. from five or six independent patch experiments as indicated.

expressing homomeric GluK2 receptors (Online Methods). Using an ultrafast agonist-perfusion system, we recorded single-channel events and then selected, for analysis, recordings in which most responses corresponded to the conductance expected of a single channel[24]. Although the actual number of active receptors per patch is not known, these single-channel recordings nevertheless reveal the different routes taken by KARs before entering into desensitization. In most cases, rapid application of saturating glutamate (10 mM L-glutamate) activated GluK2 receptors, which open to one of several conductance levels (**Fig. 1a–c**). Once in the open state, KAR channels typically closed within tens of milliseconds and did not reopen for any measurable duration of time afterwards, thus indicating that the receptor desensitized. Because desensitization is not thought to occur directly from the open state, it presumably proceeded shortly after channel closure. In agreement with this latter point, ensemble averages of single-channel sweeps exhibited decay time constants (6.49 ± 0.41 ms, n = 6; **Fig. 1d,e**) that were statistically indistinguishable from decay rates of macroscopic responses (6.28 ± 0.43 ms, n = 9, P = 0.74), thus reaffirming that the onset of KAR desensitization is approximated by the duration of channel activity.

In some cases, 10 mM L-glutamate failed to elicit a measurable response during the entire 250-ms application (**Fig. 1a**) corresponding to about 31.7 ± 5.5% of the 525 total sweeps from five patches (**Fig. 1e**). The apparent failure to respond to the agonist may reflect an intrinsic inability of L-glutamate to reliably convert its energy of binding to activation. If this was the case, however, channel opening would eventually be observed, as the continued presence of L-glutamate would ensure that the energy threshold for activation would be overcome. Consequently, the inability of L-glutamate to activate GluK2 receptors must represent the onset of desensitization without prior passage through the open state(s).

The discrete molecular events that bring about desensitization are currently unresolved. Several studies, however, identify the LBD dimer interface[15] and the cation-binding site[19,25] as taking part in the conformational events that initiate KAR macroscopic desensitization. Whether one site or the other has a more direct effect on desensitization has yet to be directly studied. As discussed below, we examined this by studying the single-channel properties of two apparently nondesensitizing GluK2 receptors, namely the mutants D776K and Y521C L783C.

The D776K mutation abolishes GluK2 receptor desensitization

The LBD dimer interface of wild-type GluK2 receptors contains binding sites for two sodium ions and a single chloride ion (**Fig. 2a**)[20,21]. Both GluK2 receptor mutations (D776K and Y521C L783C) are also located at the LBD dimer interface (**Fig. 2b,c**), where they are proposed to eliminate desensitization by constraining subunit movement. The positively charged lysine of D776K establishes new interprotomer contacts by tethering to the cation-binding pocket (**Fig. 2b**)[25], whereas the cysteine residues of Y521C L783C are thought to achieve this through the formation of covalent disulfide bridges between subunits (**Fig. 2c**)[15]. Because both mutant receptors are expected to affect the functional properties of KARs similarly, we were surprised to observe that their single-channel behavior was quite different.

Like wild-type receptors, single D776K channels were rapidly activated by 10 mM L-glutamate. However, instead of opening only briefly before desensitization, agonist binding led to sustained activation of the 21–22 pS main open state (i.e., most frequented) (**Fig. 2d**). In support of this, repetitive applications of 10 mM L-glutamate to patches containing a single D776K receptor elicited activity in every case, thus demonstrating that this mutant GluK2 receptor displays close to the maximum probability of opening. Averaged ensemble responses were nondecaying in nature with rapid off kinetics of ~2–3 ms due to L-glutamate removal (**Fig. 2d**). These persistent openings were nevertheless interrupted by transient closures too brief to represent long-lived desensitized states and which, consequently, must represent sojourns to lower conductance levels or closed or ligand-free states.

Unlike the D776K receptor, the double-cysteine mutant did not yield persistent channel activity in saturating L-glutamate. Instead, recordings were dominated by submillisecond openings that were separated by longer apparent closures (**Fig. 2e**)[26]. Given the infrequent nature of gating, we concluded that responses observed in the excised patches were likely to originate from multiple channels. Despite the transient openings, averaging sweeps from many agonist applications generated a nondecaying ensemble response. The decay kinetics of the ensemble average current of Y521C L783C receptors were nevertheless at least five times slower (14.8 ± 2.9 ms, n = 4) than those of D776K receptors (**Fig. 2e**).

For GluK2 D776K, its consistent gating behavior allowed us to make additional inferences. Time-course fitting of resolvable single-channel events estimated conductance levels of 21, 35 and 40 pS, which were

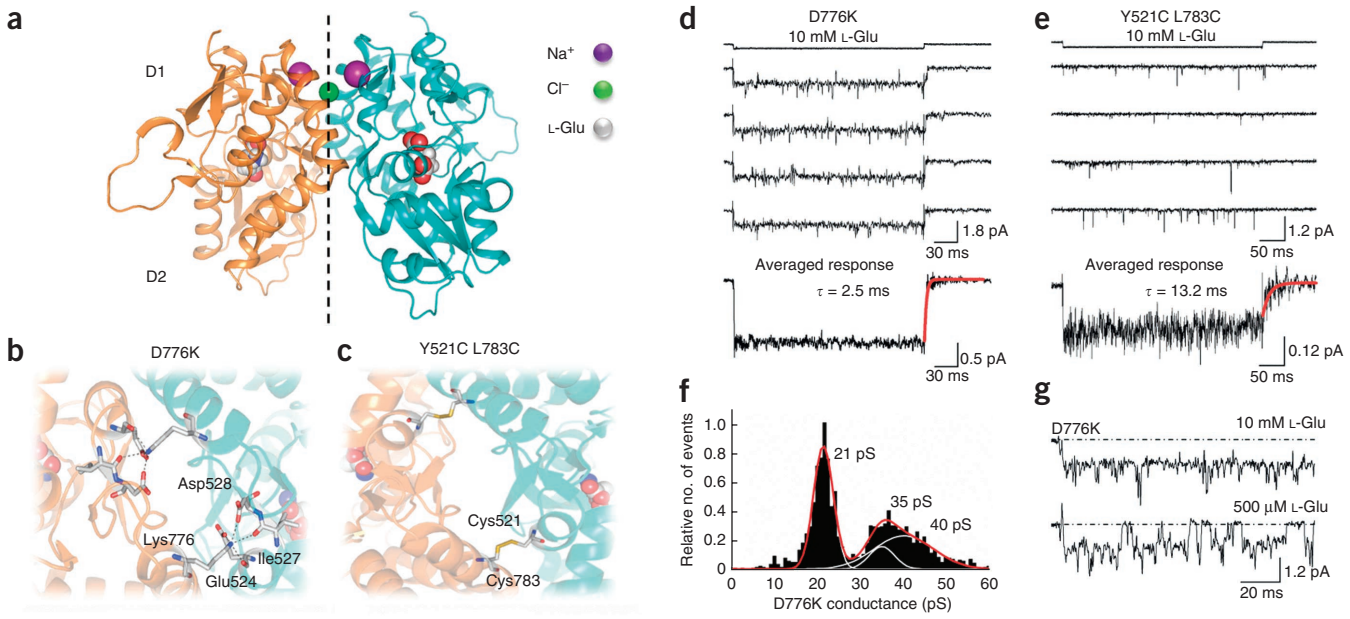

Figure 2 Mutation D776K eliminates GluK2 receptor desensitization. (**a**) Crystal structure of the wild-type GluK2 LBD dimer (PDB 3G3F[42]), including the upper (D1) and lower (D2) domains. (**b**) Top view of the GluK2 D776K LBD dimer interface showing electrostatic interactions between Lys776 and the adjacent subunit (PDB 2XXX[25]). (**c**) Top view of the GluK2 Y521C L783C LBD dimer interface showing covalent cross-linking between subunits (PDB 2I0C[15]). (**d**) Typical current responses elicited by L-glutamate acting on a single D776K channel (patch no. 12127p2, –60 mV). (**e**) Unitary current events elicited by L-glutamate acting on Y521C L783C channels (patch no. 12322p3, –100 mV). In **d** and **e**, averaged ensemble responses were taken from 20 or 95 individual current records, respectively. Time constants of deactivation were obtained by fitting agonist-off current responses with a single exponential function. (**f**) GluK2 D776K conductance distributions plotted after time-course fitting. (**g**) Individual current responses of a single GluK2 D776K receptor to 10 mM and 500 µM L-glutamate (patch no. 12124p1).

calculated by a measured reversal potential of 0 mV (**Fig. 2f**). The open level most frequently visited was 21–22 pS, closely matching the predominant 19-pS conductance level of wild-type receptors, with the two largest conductance levels corresponding to brief sojourns from this state (i.e., 35 and 40 pS). Fitting Gaussian functions to an all-points histogram of D776K data further shows that >90% of the analyzed records corresponded to the main open state (**Supplementary Fig. 1**). These conductance levels are likely to originate from single channels rather than from several channels opening simultaneously, as lowering the concentration of L-glutamate interrupted openings to the 21- to 22-pS state with clear closures to baseline (**Fig. 2g**).

In summary, our single-channel data reveal that GluK2 D776K exhibits all the hallmarks expected of a nondesensitizing KAR: sustained activation, high unitary conductance and an absence of long-duration closures. GluK2 Y521C L783C responds quite differently, and therefore we could conclude that the structural basis of its functional behavior must be different. Because the Lys776 residue is proposed to act as a tethered cation[25], we reasoned that occupancy of the ion-binding pocket might be the key structural event that prevents the onset of desensitization. If true, cation interactions at the Y521C L783C receptor might therefore be unstable, and this would account for differences observed at the single-channel level. As explained below, we tested this hypothesis by using molecular dynamics (MD) simulations to estimate the residency time of sodium bound to the cation-binding pockets of both D776K and Y521C L783C receptors.

Lys776 substitutes for sodium at the cation-binding pocket

We used MD simulations to explore how electrostatic interactions affect occupancy of the cation-binding pocket, a relationship that cannot be clarified with X-ray crystal structures or electrophysiology. Over the course of each of two 100-ns simulations, the cation pockets of the D776K receptor first released both sodium ions and then formed new contact points with the amino groups of Lys776 (**Fig. 3a–d** and **Supplementary Movie 1**). Consequently, the cation-binding pocket was nearly continuously occupied by a positive charge during the entire simulation period, a result consistent with previous structural data[25]. In contrast, simulations of the Y521C L783C receptor predict that these mutations destabilize sodium- and chloride-ion binding, thus facilitating rapid ion release in both simulations performed (**Supplementary Fig. 2a**,**b** and **Supplementary Movie 2**). There was also a tendency for water molecules to more readily occupy the cation pockets of Y521C L783C, and this may explain the instability in sodium- and chloride-ion binding. Measurements of the surface area accessible to solvent indicated a much higher propensity for water molecules to interact with residues lining the cation pocket in the double-cysteine mutant compared to wild-type GluK2 receptors (**Supplementary Fig. 2c**,**d**). If these simulations reflect the physiological behavior of kainate receptors, then activation could depend on the occupancy of the cation pocket, and cation unbinding would promote channel closure and/or desensitization.

GluK2 D776K receptors activate without external cations

If occupancy of the cation-binding pocket is a prerequisite for wild-type KAR activation, removal of all external ions should result in the absence of any detectable current. Although such recordings have already been shown to abolish wild-type KAR activity[22], this original finding has been disputed by more recent work claiming residual channel activity in ion-free conditions[21]. To re-examine this issue, we repeated experiments comparing GluK2 receptors in the presence and absence of external ions. If Lys776 acts as a tethered cation, as suggested by MD simulations (**Fig. 3**) and structural data[25], we reasoned that the GluK2 D776K would gate in the absence of

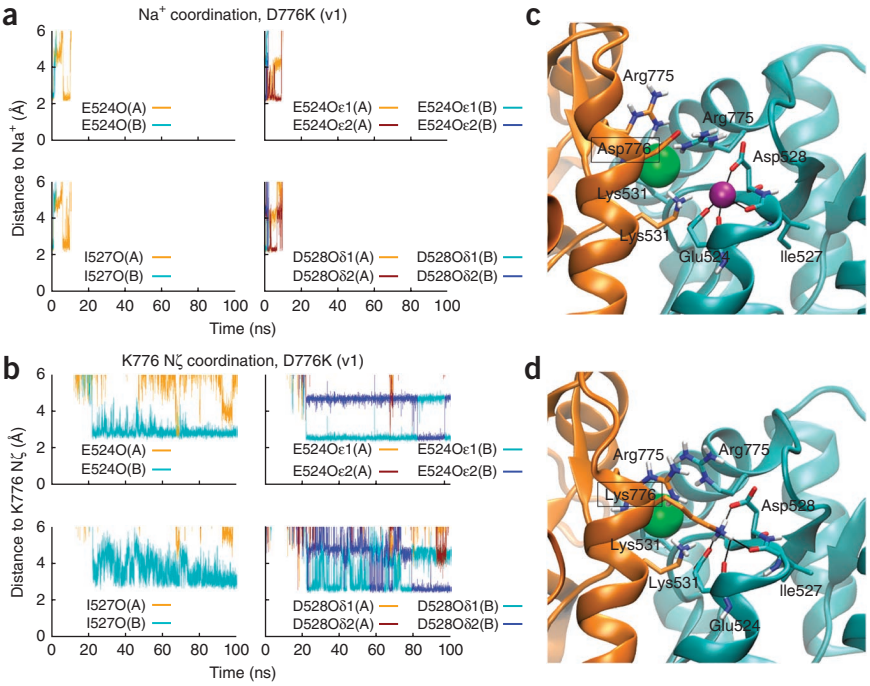

Figure 3 Lys776 can act as a tethered ion at the GluK2 cation-binding pocket. (**a**) Coordination distances between sodium ions (bound to chains A and B) and several oxygen atoms found on residues lining the cation-binding pocket (E524, I527 and D528) during a 100-ns MD simulation (version or repeat 1, v1) of the D776K mutant. (**b**) Coordination distances for the positively charged Nζ of Lys776 (simulation repeat 1, v1). Distances were measured from oxygen atoms normally involved in sodium ion coordination. (**c**) Sodium ion coordination in the crystal structure of wild-type GluK2 LBD. (**d**) Snapshot after 100 ns of MD simulation of the D776K mutant. Orange, chain A and its residues; cyan, chain B and its residues; purple, sodium ion; green, chloride ion. Coordination distances are indicated with black lines for the sodium ion (**c**) and the Lys776 amine (**d**). Water molecules and nonpolar hydrogen atoms are omitted. Black boxes surround mutated residues.

external cations. In contrast, the instability of cation binding to GluK2 Y521C L783C suggests that this mutant would fail to gate in the absence of ions unless cross-linking of the LBD dimer interface permits activation through a different mechanism. Consistent with the above predictions, wild-type GluK2 receptor activity was completely abolished by the removal of external monovalent ions (**Fig. 4a**,**b**), whereas the D776K receptor continued to gate (**Fig. 4c**,**d**), thus demonstrating that the wild-type GluK2 receptor gating mechanism has an absolute requirement for external cations. These data also further support the idea that the Lys776 residue acts as a tethered cation, thus accounting for the ability of the D776K receptor to gate in the absence of external ions.

Interestingly, the Y521C L783C receptor was also able to gate in the absence of external cations (**Fig. 4e**,**f**). This finding is in agreement with a prior study[21] but is inconsistent with the lack of responsiveness of wild-type GluK2 receptors in ion-free conditions (**Fig. 4a**,**b**), thus suggesting the need for an alternative explanation. With this in mind, we considered the possibility that cross-linking of the dimer interface of the GluK2 receptor may eliminate the requirement of external cations for activation. We tested this possibility by identifying mutations in the LBD dimer interface that would disrupt cation binding without forming interprotomer cross-links.

Destabilizing cation binding impairs GluK2 activation

We studied disruption of the cation-binding pocket by examining two mutant receptors, namely GluK2 E524G and L783C, which MD simulations suggest destabilize sodium binding to the cation-binding pocket. Importantly, these mutations do not affect receptor surface expression (**Supplementary Fig. 3a**,**b**). For E524G, which has a less electronegative cation pocket, two 50-ns simulations of sodium coordination both estimated that sodium is released within 5 ns. In contrast, the wild-type receptor retained sodium for the duration of two 100-ns

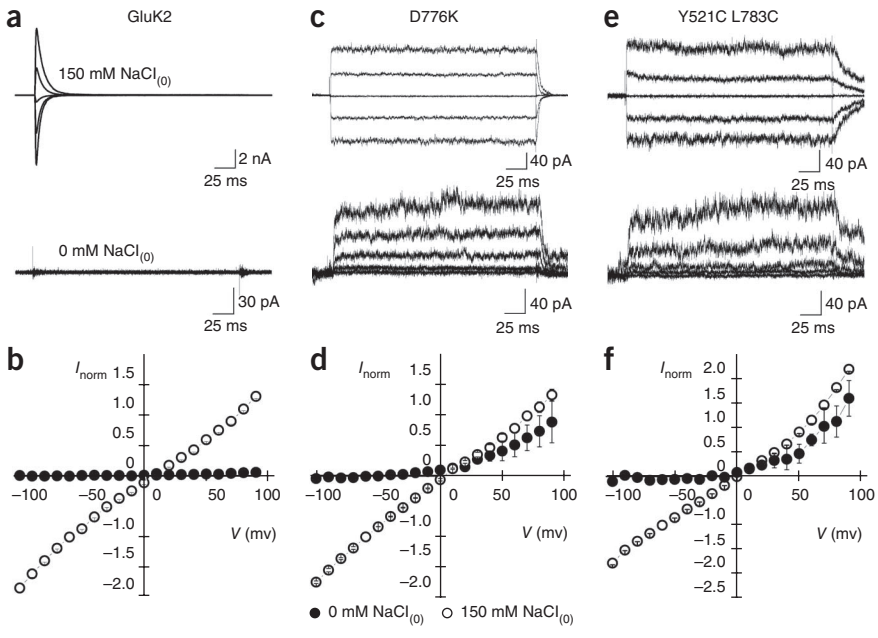

Figure 4 GluK2 D776K receptors gate in the absence of external ions. (**a**,**c**,**e**) Membrane currents evoked by L-glutamate acting on wild-type GluK2 (**a**), D776K (**c**) and Y521C L783C (**e**) receptors, in either 150 mM NaCl (top) or in nominal ion-free (bottom) external solution (V_m = –60, –30, 0, 30 and 60 mV). For wild-type GluK2, the same patch was recorded in both ionic conditions (patch no. 121106p2). Mutant responses were taken from different patches (D776K ion, patch no. 11510 p1; ion free, patch no. 12925p5; Y521C L783C ion, patch no. 121002p2; ion free, patch no. 121023p2). (**b**,**d**,**f**) Averaged current (I_{norm})-voltage (V) plots in 0 mM (filled circles) and 150 mM (open circles) NaCl for wild-type GluK2 (**b**), D776K (**d**) and Y521C L783C (**f**) receptors. Currents were normalized to responses at –60 mV in 150 mM NaCl. Error bars, s.e.m. from three independent experiments for each receptor.

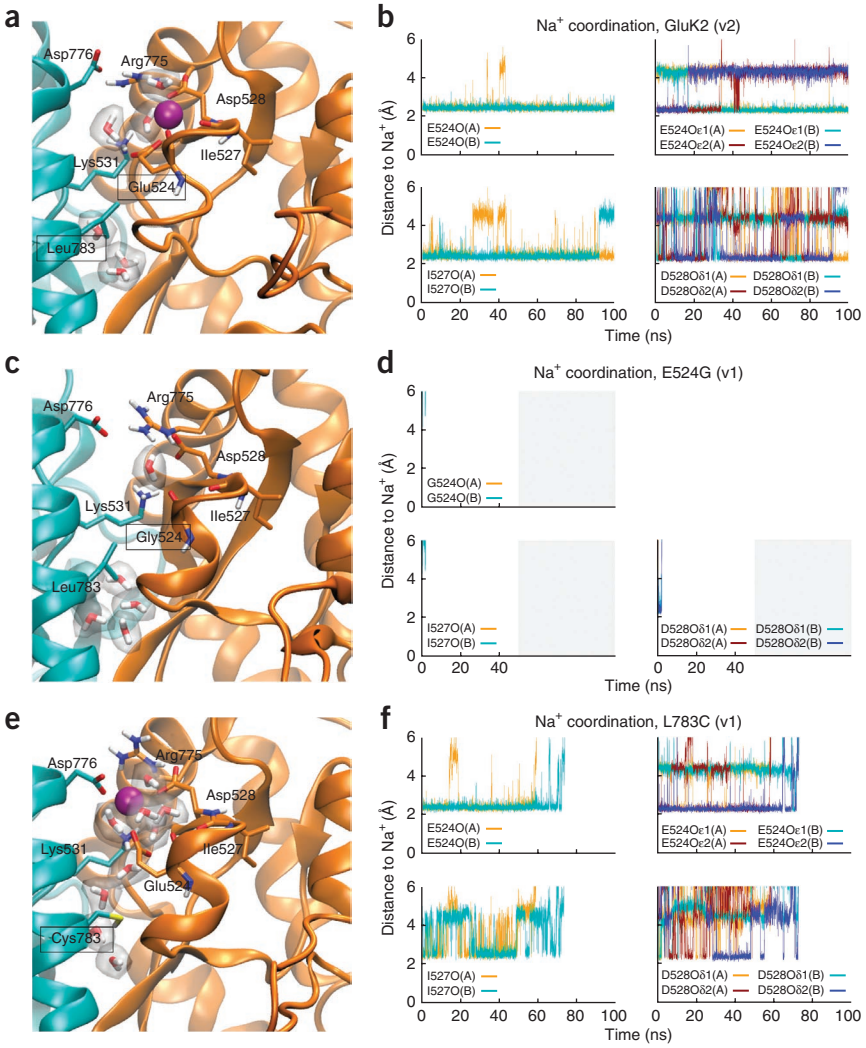

Figure 5 Occupancy of the GluK2 cation-binding pocket is predicted to be disrupted by targeted mutation of the dimer interface. (**a**,**c**,**e**) Snapshots of sodium coordination in the wild-type GluK2 receptor (**a**), as well as mutants E524G (**c**) and L783C (**e**), all taken ~15 ns after the start of the MD simulation. Black boxes surround mutated residues. (**b**,**d**,**f**) Sodium coordination plotted from MD simulations of the LBD dimer in the wild-type GluK2 receptor, repeat 2, v2 (**b**) and mutants E524G, repeat 1, v1 (**d**) and L783C, repeat 1, v1 (**f**).

simulations (**Fig. 5a–d** and **Supplementary Movies 3** and **4**). In this respect, E524G mimics the Y521C L783C receptor; however, it differs in that 10 mM L-glutamate fails to elicit a measurable response in most excised patches (**Supplementary Fig. 3c**). We did observe responses in 3 out of the 18 patches tested, but they were small (<10 pA at −60 mV) in amplitude and thus consistent with the E524G mutation acting to destabilize cation binding.

Interestingly, when only one of the cross-linking residues (i.e., L783C) was mutated, 10 mM L-glutamate failed to elicit a response in all cases, whether we examined whole-cell recordings (B.A.D. and D.B., unpublished data) or excised patches (n = 15) (**Supplementary Fig. 3c**). MD simulations suggested that the L783C mutant has a less pronounced effect than does E524G on sodium stability, yet the ions managed to dissociate from their binding pockets within 100 ns in one of two simulations (**Fig. 5e**,**f**). One potential explanation for the sodium dissociation is that the L783C mutant permits access of additional water molecules into the cation-binding pocket (**Supplementary Movie 5**), as observed in simulations of Y521C L783C. In comparison to the wild-type GluK2 receptor, the sodium ions in L783C interacted more frequently with water molecules and less frequently with residues of the cation pocket (M.M. and P.C.B., unpublished data). In both mutants, our data point to the lack of responsiveness of E524G and L783C arising from their disruptive effects on the cation-binding pocket, a condition that may be similar to desensitization in a wild-type receptor. Because mutant receptors that disrupt L-glutamate binding are retained within mammalian cells[27], we do not think that an inability to bind agonists can account for the phenotypes of E524G and L783C. As a result, an explanation is required to account for an additional cysteine (Y521C) restoring channel gating when introduced atop the L783C mutation. We conclude that the cation-independent activation of GluK2 Y521C L783C is due to its covalent cross-linking of the dimer interface circumventing the normal gating requirements of the wild-type receptor (additional information in ref. 26).

KAR desensitization proceeds after cation unbinding

MD simulations and single-channel data suggest that GluK2 D776K receptors are nondesensitizing, because Lys776 becomes tethered to the cation-binding pocket. We therefore conclude that cation binding primes KARs for activation by the agonist. We also conclude that cation-unbound states are not primed for activation, and thus agonist binding promotes entry into desensitized states, as observed with the L783C and E524G mutant receptors. These different outcomes are important because they will determine the degree to which desensitization, and by implication cation unbinding, contributes to the wild-type KAR response. For example, during long agonist applications routinely used to measure desensitization rates, most receptors should desensitize because cations will eventually unbind with the agonist still bound. In contrast, with brief applications of L-glutamate used to measure deactivation rates, fewer GluK2 receptors should desensitize, because the agonist will unbind before the cation. Importantly, this sequence of events can be tested experimentally. Specifically, we predict that deactivation rates estimated with a brief agonist application should be minimally affected by the presence or absence of desensitization because decay from the peak response corresponds to agonist unbinding from the cation-bound state(s).

To examine the impact of desensitization on deactivation rates, we compared the relaxation kinetics observed after a brief application (i.e., 1 ms) of 10 mM L-glutamate onto wild-type and nondesensitizing D776K KARs (**Fig. 6a**). For comparison, we also performed a similar analysis of wild-type and a mutant GluA1 AMPA receptor (i.e., L497Y) in which single-channel desensitization is strongly inhibited[28] (**Fig. 6b**). Wild-type GluK2 receptors exhibited a fast exponential time constant of deactivation of 2.3 ± 0.1 ms (n = 7) (**Fig. 6a**), which was statistically indistinguishable from the off kinetics of

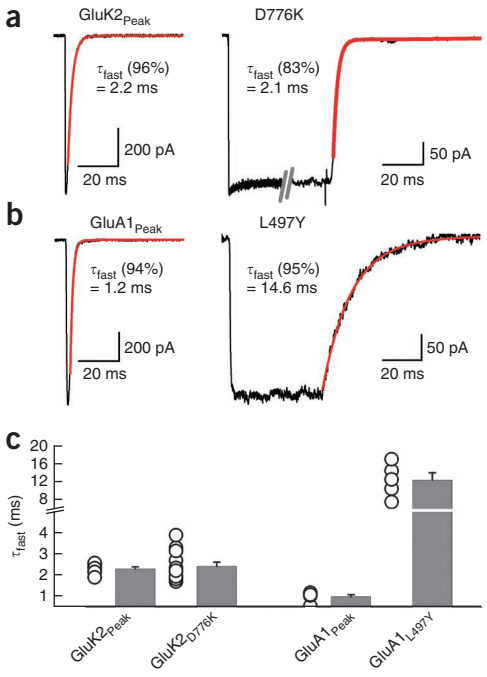

Figure 6 Desensitization and deactivation are uncoupled in GluK2 KARs. (**a**) Typical current decay observed after removal of 10 mM L-glutamate from wild-type GluK2 (1-ms application, patch no. 00327p3) and GluK2 D776K (250-ms application, patch no. 11506p1) receptors. (**b**) Typical current decay observed after removal of 10 mM L-glutamate from wild-type GluA1 (1-ms application, patch no. 00404p1, –55 mV) and GluA1 L497Y (50-ms application, patch no. 99608p1, –55 mV) receptors. For **a** and **b**, decay kinetics from saturating L-glutamate were fit with a second-order exponential function (red) with representative values of the fast, dominant component displayed. (**c**) Distribution of off-kinetic rates show that the τ_{fast} values for the GluK2 peak response and D776K were statistically indistinguishable (described in text), whereas the values for the GluA1 peak response and L497Y were statistically different ($P < 0.001$ by two-tailed Student's t test ($\alpha = 0.05$)). Error bars, s.e.m. from seven (GluK2), twelve (D776K), six (GluA1) or five (L497Y) independent experiments.

D776K receptors regardless of whether 1-ms (2.0 ± 0.2 ms, $n = 9$; $P = 0.63$) or 250-ms agonist pulses (2.4 ± 0.2 ms, $n = 12$; $P = 0.82$) were applied (**Fig. 6a**,**c**). These observations support our assertion that KAR desensitization proceeds after cation unbinding. Accordingly, deactivation and desensitization can therefore be viewed as being structurally distinct and separable processes. In contrast, the decay time constant observed after a 1-ms application of 10 mM L-glutamate to GluA1 AMPARs had a fast exponential time constant of 1.0 ± 0.1 ms ($n = 6$) (**Fig. 6b**), which was about 10 times faster than the off kinetics of the nondesensitizing L497Y mutant (12.4 ± 1.6 ms, $n = 5$; **Fig. 6b**,**c**). This finding is consistent with the effect of the allosteric modulator cyclothiazide, which also attenuates AMPAR desensitization[29].

To further test the impact of desensitization on the activation process, we compared the dose-response relationships of GluK2 D776K and wild-type receptors. We reasoned that because the absence of desensitization had little to no effect on GluK2 deactivation kinetics, rates of L-glutamate unbinding should be high relative to rates of cation unbinding, which equate with desensitization. Under such circumstances, receptors would tend to enter desensitized states only during sustained L-glutamate application. As such, the dose-response relationship of the peak response, occurring less than 1 ms after L-glutamate exposure, should exhibit little change in the absence of desensitization.

In agreement with our predictions, the half-maximal effective concentration (EC_{50}) (and Hill coefficient, n_H) estimated from peak dose-response curves to L-glutamate acting on wild-type GluK2 receptors

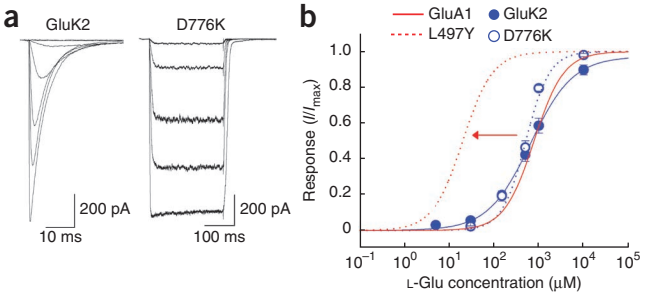

Figure 7 Desensitization does not substantially shift peak agonist potency of GluK2 KARs. (**a**) Typical current responses elicited by L-glutamate (10 μM–10 mM) acting on wild-type GluK2 (patch no. 091204p2) and GluK2 D776K (patch no. 11610p1) receptors. (**b**) L-glutamate dose-response relationships for KARs, normalized to the maximal current (I_{max}) of each patch, as well as simulated dose-response curves of wild-type and GluA1 L497Y receptors taken from previously reported values[29]. Error bars, s.e.m. from seven (GluK2) and eight (D776K) independent experiments.

was 652 ± 47 μM ($n_H = 0.87$, $n = 7$), which closely matched that of D776K receptors, whose EC_{50} values were estimated to be 520 ± 91 μM ($n_H = 1.6$, $n = 8$) (**Fig. 7a**,**b**). These data differ from past work on AMPARs, which has shown that mutations and allosteric modulators that reduce or eliminate desensitization cause progressive leftward shifts in the wild-type dose-response curve[28,29]. For example, one study noted a leftward shift of over an order of magnitude from the wild-type EC_{50} to that of GluA1 L497Y[29] (**Fig. 7b**). Our observations comparing wild-type and D776K receptors support the idea that desensitization has little impact on the time GluK2 receptors remain activated. This is, of course, to be expected if desensitization can proceed only after cation unbinding. Indeed, MD simulations reported here suggest that LBD dimer separation, a structural correlate of desensitization, is promoted for wild-type receptors in the absence of bound sodium ions (**Supplementary Fig. 4**). Our findings also suggest that desensitization affects the time course of AMPAR activation, and this explains the effect of desensitization on both deactivation kinetics and agonist potency.

DISCUSSION

The present study advances the understanding of iGluR gating in several ways. First, we show that cation occupancy is the central requirement in keeping agonist-bound KARs in the activated state and out of desensitization. Second, we propose a structural model for the sequence of events that give rise to deactivation and desensitization. Deactivation is observed when the ligand unbinds from cation-bound states, whereas desensitization proceeds when the ligand is bound to cation-unbound states. Third, and finally, closely related AMPARs do not share this reliance on cation-dependent gating; as a result, desensitization appears able to curtail AMPAR channel activation. As discussed below, this unique property of KARs may provide clues as to how subunit composition and/or auxiliary proteins affect native receptors at glutamatergic synapses.

The KAR dimer interface is a multifaceted structure

It is remarkable that subunit cross-linking at two neighboring sites (residues 776 and 783) along the GluK2 LBD dimer interface produces

very different functional consequences. The Y521C L783C mutation bridges opposing subunits, yet the crystal structure of its LBD suggests a separation of the upper D1 segment of the dimer interface[15]. Although separation of the dimer interface is thought to underlie both KAR and AMPAR desensitization[13], it is not clear how much separation would be tolerable before channel activation could no longer be maintained. Given microscopic recordings showing that Y521C L783C channels cannot stably access the main open state of wild-type GluK2 (ref. 26), we propose that this mutant is a mostly desensitized receptor typified by an open interface and/or a poorly activating receptor by virtue of its sporadic channel openings.

Targeted slightly higher along the LBD interface, the mutant residue Lys776 occupies the GluK2 cation-binding pocket and has two related consequences on receptor function: it increases open-channel probability to such an extent that no failures are observed, and it sustains activation for the duration of agonist application. The latter effect supports the idea that the molecular events leading to desensitization are triggered at the apex of the interface rather than being coordinated through the interface as a whole. Whether these interactions are further complicated according to an emerging idea that KAR subunits desensitize with a tetrameric symmetry and not as a dimer of dimers[30,31] awaits future study.

The cation-binding pocket and its relation to gating events

Although structural rearrangements of the LBD accompany iGluR desensitization[13], it is presently unknown how such conformational changes are initiated. The matter is further complicated in KARs, in which bound ions have been proposed to stabilize the LBD dimer interface[20]. Here, we establish a framework to specify when KARs activate and desensitize by identifying the cation-binding pocket as the molecular switch between these processes. In short, cation pocket occupancy maintains KAR activation, and by implication desensitization cannot occur until cations unbind. The link between cation binding and activation is based on several key observations reported above: the sustained single-channel activation in the GluK2 D776K mutation (**Fig. 2**), in which the cation-binding pocket is thought to be continuously occupied; the inability of GluK2 to activate in the absence of external ions (**Fig. 4**); and the gating deficiencies among mutants designed to disrupt cation binding (**Fig. 5** and **Supplementary Fig. 3**). Furthermore, the assertion that cation unbinding precedes desensitization can be deduced from other observations we reported. Specifically, we showed that deactivation kinetics of wild-type KARs were unaffected by desensitization, thus confirming our assertion that the decay of the KAR peak response corresponds to agonist unbinding from the cation-bound state(s) (**Fig. 6a**,**c**). This conclusion is consistent with previous work showing that GluK2 deactivation kinetics are made faster by lowering of the external cation concentration or replacement of sodium with another cation[32]. With long agonist applications (i.e., 250 ms), we propose that the decline in KAR activity is due to cation unbinding because besides the presence of the agonist, the only other known requirement of KARs to activate is allosteric ions[22]. Given this, we concluded that their departure was the most plausible explanation to trigger the onset of desensitization. In accordance with this notion, MD simulations reported here (**Supplementary Fig. 4**) predict that removal of cations from the LBD dimer interface can induce structural changes associated with the desensitized state(s).

An alternative explanation for the observations above is that KAR desensitization is triggered by intrinsic rearrangements to the LBD structure, which are countered through the occupancy of bound cations. From this perspective, the relation between bound cations and decay kinetics is attributable to a direct modulation of the intrinsic rate of desensitization (by stabilization of LBD dimers), as has been suggested previously[21]. This interpretation, however, is difficult to reconcile with several observations. To begin with, if desensitization is merely opposed but not blocked by the presence of bound cations, some residual activation should be detected in solutions lacking external ions, but this is not the case. Furthermore, from this perspective, the effect of cation species on deactivation kinetics would have to be explained by desensitization rates overlapping with those of deactivation. Experiments reported here show that deactivation kinetics are unaffected by desensitization (i.e., comparison of D776K to wild-type GluK2 receptors) (**Fig. 6**), meaning that desensitization must therefore occur on a slower time scale. Thus, the two processes do not overlap, and activation must be directly regulated by cations.

Ion channels use different strategies to desensitize

Desensitization of LGICs has been classically thought to arise from agonist molecules converting receptor complexes into nonreactive forms[33], in much the same way that even earlier work linked changes in membrane potential to voltage-gated ion-channel inactivation[34]. Since then, structural explanations have emerged to account for how the processes of inactivation and desensitization occur at the amino acid level. Some of the first insights came from work on voltage-gated sodium and potassium channels, which were shown to possess intracellular inactivation gates[35,36], whereas work on cysteine-loop LGICs hinted at a broader rearrangement of quaternary structure[37]. Pioneering studies also identified coupling between activation and inactivation of voltage-gated channels[38], although this coupling has been more difficult to establish at LGICs. Such coupling might be expected to occur at iGluRs because closure in the agonist-binding domain initiated by ligand binding is thought to bring about both activation and subsequent desensitization, as the agonist becomes entrapped in a stable yet inactive conformation[12,39]. In keeping with this, data presented in this study suggest a tight coupling between these structural events in AMPARs. Interestingly, this is not the case for KARs, which uncouple the process of activation from desensitization through cation-dependent gating. This unique aspect of KAR gating provides an ideal target by which native receptor responses could be modulated at central synapses. For example, alterations in cation affinity through protein-protein interactions could explain how heteromeric subunits[40] and/or auxiliary proteins[24] regulate the duration of synaptic KAR activity[41]. Clearly, much still remains to be examined in future studies, including how this allosteric cation-binding pocket might be exploited to regulate KAR signaling within the vertebrate central nervous system.

METHODS

Methods and any associated references are available in the online version of the paper.

Note: Any Supplementary Information and Source Data files are available in the online version of the paper.

ACKNOWLEDGMENTS

This work was supported by operating grants from the Canadian Institutes of Health Research (CIHR) FRN-82804 (D.B.) and by the Leverhulme Trust RPG-059 (P.C.B.). G.B.D. and E.D.A. were supported by Natural Sciences and Engineering Research Council of Canada graduate fellowships, B.A.D. by a Chemical Biology CIHR postdoctoral award and M.R.P.A. by a CIHR Best & Banting doctoral award. D.B. is supported by a Canada Research Chair award. We thank the Oxford Supercomputing Centre for computer time. Finally, we wish to thank J. Johnson for comments on the manuscript and M. Fleck for discussions on AMPA receptors.

AUTHOR CONTRIBUTIONS

G.B.D. designed and performed experiments, analyzed data and wrote the paper; M.M., B.A.D. and M.R.P.A. designed and performed experiments and analyzed

data; E.D.A. analyzed data; P.C.B. designed experiments; and D.B. designed and performed experiments, analyzed data and wrote the paper.

COMPETING FINANCIAL INTERESTS
The authors declare no competing financial interests.

1. Katz, B. & Thesleff, S. A study of the desensitization produced by acetylcholine at the motor end-plate. *J. Physiol.* (*Lond.*) **138**, 63–80 (1957).
2. Shelley, C. & Cull-Candy, S.G. Desensitization and models of receptor-channel activation. *J. Physiol.* (*Lond.*) **588**, 1395–1397 (2010).
3. Jones, M.V. & Westbrook, G.L. The impact of receptor desensitization on fast synaptic transmission. *Trends Neurosci.* **19**, 96–101 (1996).
4. Hille, B. *Ion Channels of Excitable Membranes* 169–200 (Sinauer Associates, 2001).
5. Patneau, D.K., Mayer, M.L., Jane, D.E. & Watkins, J.C. Activation and desensitization of AMPA/kainate receptors by novel derivatives of willardiine. *J. Neurosci.* **12**, 595–606 (1992).
6. Traynelis, S.F. *et al.* Glutamate receptor ion channels: structure, regulation, and function. *Pharmacol. Rev.* **62**, 405–496 (2010).
7. Corringer, P.J. *et al.* Structure and pharmacology of pentameric receptor channels: from bacteria to brain. *Structure* **20**, 941–956 (2012).
8. Flynn, G.E., Johnson, J.P. Jr. & Zagotta, W.N. Cyclic nucleotide-gated channels: shedding light on the opening of a channel pore. *Nat. Rev. Neurosci.* **2**, 643–651 (2001).
9. Hansen, K.B., Yuan, H. & Traynelis, S.F. Structural aspects of AMPA receptor activation, desensitization and deactivation. *Curr. Opin. Neurobiol.* **17**, 281–288 (2007).
10. Wollmuth, L.P. & Sobolevsky, A.I. Structure and gating of the glutamate receptor ion channel. *Trends Neurosci.* **27**, 321–328 (2004).
11. Madden, D.R. The structure and function of glutamate receptor ion channels. *Nat. Rev. Neurosci.* **3**, 91–101 (2002).
12. Armstrong, N., Sun, Y., Chen, G.Q. & Gouaux, E. Structure of a glutamate-receptor ligand-binding core in complex with kainate. *Nature* **395**, 913–917 (1998).
13. Sun, Y. *et al.* Mechanism of glutamate receptor desensitization. *Nature* **417**, 245–253 (2002).
14. Armstrong, N., Jasti, J., Beich-Frandsen, M. & Gouaux, E. Measurement of conformational changes accompanying desensitization in an ionotropic glutamate receptor. *Cell* **127**, 85–97 (2006).
15. Weston, M.C., Schuck, P., Ghosal, A., Rosenmund, C. & Mayer, M.L. Conformational restriction blocks glutamate receptor desensitization. *Nat. Struct. Mol. Biol.* **13**, 1120–1127 (2006).
16. Priel, A., Selak, S., Lerma, J. & Stern-Bach, Y. Block of kainate receptor desensitization uncovers a key trafficking checkpoint. *Neuron* **52**, 1037–1046 (2006).
17. Gielen, M. *et al.* Structural rearrangements of NR1/NR2A NMDA receptors during allosteric inhibition. *Neuron* **57**, 80–93 (2008).
18. Borschel, W.F., Murthy, S.E., Kasperek, E.M. & Popescu, G.K. NMDA receptor activation requires remodelling of intersubunit contacts within ligand-binding heterodimers. *Nat. Commun.* **2**, 498 (2011).
19. Nayeem, N., Zhang, Y., Schweppe, D.K., Madden, D.R. & Green, T. A nondesensitizing kainate receptor point mutant. *Mol. Pharmacol.* **76**, 534–542 (2009).
20. Plested, A.J. & Mayer, M.L. Structure and mechanism of kainate receptor modulation by anions. *Neuron* **53**, 829–841 (2007).
21. Plested, A.J., Vijayan, R., Biggin, P.C. & Mayer, M.L. Molecular basis of kainate receptor modulation by sodium. *Neuron* **58**, 720–735 (2008).
22. Wong, A.Y., Fay, A.M. & Bowie, D. External ions are coactivators of kainate receptors. *J. Neurosci.* **26**, 5750–5755 (2006).
23. Bowie, D. Ion-dependent gating of kainate receptors. *J. Physiol.* (*Lond.*) **588**, 67–81 (2010).
24. Zhang, W. *et al.* A transmembrane accessory subunit that modulates kainate-type glutamate receptors. *Neuron* **61**, 385–396 (2009).
25. Nayeem, N., Mayans, O. & Green, T. Conformational flexibility of the ligand-binding domain dimer in kainate receptor gating and desensitization. *J. Neurosci.* **31**, 2916–2924 (2011).
26. Daniels, B.A., Andrews, E.D., Aurousseau, M.R., Accardi, M.V. & Bowie, D. Crosslinking the ligand-binding domain dimer interface locks kainate receptors out of the main open state. *J. Physiol.* (*Lond.*) http://dx.doi.org/10.1113/jphysiol.2013.253666 (27 May 2013).
27. Mah, S.J., Cornell, E., Mitchell, N.A. & Fleck, M.W. Glutamate receptor trafficking: endoplasmic reticulum quality control involves ligand binding and receptor function. *J. Neurosci.* **25**, 2215–2225 (2005).
28. Stern-Bach, Y., Russo, S., Neuman, M. & Rosenmund, C. A point mutation in the glutamate binding site blocks desensitization of AMPA receptors. *Neuron* **21**, 907–918 (1998).
29. Mitchell, N.A. & Fleck, M.W. Targeting AMPA receptor gating processes with allosteric modulators and mutations. *Biophys. J.* **92**, 2392–2402 (2007).
30. Bowie, D. & Lange, G.D. Functional stoichiometry of glutamate receptor desensitization. *J. Neurosci.* **22**, 3392–3403 (2002).
31. Schauder, D.M. *et al.* Glutamate receptor desensitization is mediated by changes in quaternary structure of the ligand binding domain. *Proc. Natl. Acad. Sci. USA* **110**, 5921–5926 (2013).
32. Bowie, D. External anions and cations distinguish between AMPA and kainate receptor gating mechanisms. *J. Physiol.* (*Lond.*) **539**, 725–733 (2002).
33. Del Castillo, J. & Katz, B. Interaction at end-plate receptors between different choline derivatives. *Proc. R. Soc. Lond. B Biol. Sci.* **146**, 369–381 (1957).
34. Hodgkin, A.L. & Huxley, A.F. The dual effect of membrane potential on sodium conductance in the giant axon of *Loligo*. *J. Physiol.* (*Lond.*) **116**, 497–506 (1952).
35. Hoshi, T., Zagotta, W.N. & Aldrich, R.W. Biophysical and molecular mechanisms of Shaker potassium channel inactivation. *Science* **250**, 533–538 (1990).
36. Stühmer, W. *et al.* Structural parts involved in activation and inactivation of the sodium channel. *Nature* **339**, 597–603 (1989).
37. Unwin, N., Toyoshima, C. & Kubalek, E. Arrangement of the acetylcholine receptor subunits in the resting and desensitized states, determined by cryoelectron microscopy of crystallized Torpedo postsynaptic membranes. *J. Cell Biol.* **107**, 1123–1138 (1988).
38. Armstrong, C.M. & Bezanilla, F. Inactivation of the sodium channel: II. gating current experiments. *J. Gen. Physiol.* **70**, 567–590 (1977).
39. Mano, I., Lamed, Y. & Teichberg, V.I. A venus flytrap mechanism for activation and desensitization of α-amino-3-hydroxy-5-methyl-4-isoxazole propionic acid receptors. *J. Biol. Chem.* **271**, 15299–15302 (1996).
40. Barberis, A., Sachidhanandam, S. & Mulle, C. GluR6/KA2 kainate receptors mediate slow-deactivating currents. *J. Neurosci.* **28**, 6402–6406 (2008).
41. Copits, B.A. & Swanson, G.T. Dancing partners at the synapse: auxiliary subunits that shape kainate receptor function. *Nat. Rev. Neurosci.* **13**, 675–686 (2012).
42. Miesenböck, G., De Angelis, D.A. & Rothman, J.E. Visualizing secretion and synaptic transmission with pH-sensitive green fluorescent proteins. *Nature* **394**, 192–195 (1998).

ONLINE METHODS

Cell culture and transfection. HEK293T cells were transiently cotransfected with cDNA encoding wild-type or mutant GluK2(Q) KAR or GluA1(Q) AMPAR subunits and enhanced GFP ($eGFP_{S65T}$), as previously described[32], or transfected with iGluR-subunit cDNA on plasmids also encoding eGFP behind an internal ribosomal entry site. The cDNA for the mutant receptors was generated in two steps from wild-type plasmid with QuikChange II XL site-directed mutagenesis (Stratagene). After transfection for 4–8 h with the calcium phosphate precipitation method, cells were washed twice with divalent cation–containing PBS and maintained in fresh medium (MEM containing Glutamax and 10% FBS). Electrophysiological recordings were performed 24–48 h later.

GluK2 receptor surface expression. To test for possible trafficking defects in mutants used in this study, we measured the fluorescence emitted by an ecliptic $_{pH}$GFP genetically fused to the extracellular N-termini of mutant or wild-type GluK2 receptors (**Supplementary Fig. 3a**,**b**). Unlike that of eGFP, the fluorescence emission of $_{pH}$GFP is almost entirely quenched at pH 5.45 (ref. 42), which we used to evaluate the cellular location of the fluorophores[43]. With this approach, a substantial but reversible attenuation in the fluorescence signal emitted by wild-type $_{pH}$GFP-GluK2 was observed ($n = 17$ cells) after acidification of the external milieu (**Supplementary Fig. 3a**,**b**), thus demonstrating that most of the fluorescence signal was emitted by tagged GluK2 receptors on the plasma membrane. In contrast, acidification of the external solution had little effect on the weak fluorescence emitted by $_{pH}$GFP-GluK2 R523A receptors ($n = 6$ cells) (**Supplementary Fig. 3a**,**b**), consistent with previous work showing that this mutant has poor surface expression[27]. Fluorescence emitted by $_{pH}$GFP-GluK2 E524G and L783C receptors ($n = 10$ and 6 cells respectively) was robust, much like that of wild-type GluK2, and was reversibly attenuated by acidification (**Supplementary Fig. 3a**,**b**), thus suggesting that trafficking to the plasma membrane is not substantially perturbed for either mutant.

Electrophysiological solutions and recordings. External recording solutions typically contained 150 mM NaCl, 5 mM HEPES, 0.1 mM $CaCl_2$, 0.1 mM $MgCl_2$ and 2% phenol red. The internal recording solution contained 115 mM NaCl, 10 mM NaF, 5 mM HEPES, 5 mM Na_4BAPTA, 0.5 mM $CaCl_2$, 1 mM $MgCl_2$ and 10 mM Na_2ATP to chelate endogenous polyamines. The osmotic pressure was set to 295–300 mOsm with sucrose and the pH adjusted to 7.35 with 5 N NaOH. Agonist solutions were prepared by dissolving the agonist in external solution and adjusting the pH appropriately. In the case of recordings conducted in nominal external ions, the solution contained 100 μM of $CaCl_2$ and $MgCl_2$ to improve patch stability, sucrose to maintain the osmotic pressure at 295–300 mOsm, and 5 mM Tris to buffer pH. The pH was adjusted to 7.3–7.4 with 10 N HCl. To optimize recording stability in solutions of nominal ions, quartz electrodes were used to excise some outside-out patches. The outward current conveyed by receptors in such conditions was due to the efflux of sodium ions from the patch pipette. The lack of inward current in response to L-Glu confirmed that all cations were removed from the external milieu of the membrane patch.

All experiments were performed on excised membrane patches in the outside-out configuration. We used thin-walled borosilicate glass pipettes (3–5 MΩ, King Precision Glass) coated with dental wax for macroscopic experiments. To obtain low-noise or single-channel recordings, we used quartz glass (3–15 MΩ, King Precision Glass) coated with Sylgard (Dow Corning). Agonist solutions were rapidly applied to outside-out patches for 250 ms at −60 mV (unless otherwise stated) with a piezo-stack–driven perfusion system. Sufficient time between applications of L-Glu was allowed for complete recovery from macroscopic desensitization. Solution exchange time was determined routinely at the end of each experiment by measurement of the liquid junction current (10–90% rise time = 100–400 μs). Series resistances (3–15 MΩ) were routinely compensated by 95%. For microscopic recordings, the headstage was set to the capacitive feedback recording mode. All recordings were performed at room temperature with an Axopatch 200B amplifier (Axon Instruments). Current records were filtered at 5 kHz for macroscopic responses and digitized at 25–50 kHz. Single-channel currents were all acquired at 50–100 kHz, low-pass filtered by an eight-pole Bessel filter at 10 kHz and digitally filtered offline at 1–3 kHz. The reference electrode was connected to the bath through an agar bridge of 3 M KCl. Data were acquired with pClamp9 software (Axon Instruments) and illustrated with Origin 7 (OriginLab).

Macroscopic response analysis. Data were analyzed with Clampfit 9.0 and tabulated with Microsoft Excel. Curve fittings for determining the off-kinetic rates were performed with first- or second-order exponential functions: $y = A_i \times \exp(-x/t_i)$. Dose-response data to L-Glu were normalized, pooled across patches and fit with the logistic equation of the following form: $I = I_{max}/(1 + (EC_{50}/[Glu])^{n_H})$, where I is the normalized current at any agonist concentration, I_{max} is the interpolated maximal response, EC_{50} is the concentration of L-Glu that elicits the half-maximal response, and n_H is the slope or Hill coefficient.

Single-channel analysis. For wild-type GluK2 receptors, analysis was conducted on patches ($n = 5$) from which 50 or more agonist applications were made at 15-s intervals. For GluK2 D776K, which displayed uniform current responses, analysis was limited to 58 agonist applications, which were divided among four patches. Single-channel data were subjected to digital low-pass filtering at 3 kHz (or 1 kHz for presentation in figures), which resulted in r.m.s. baseline noise values that averaged 0.22 ± 0.024 pA ($n = 5$) and 0.22 ± 0.043 pA ($n = 4$) for wild-type and D776K receptors, respectively. These noise values corresponded to <50% of the smallest difference between adjacent conductance levels in the wild-type receptor. The 3-kHz frequency was chosen on account of our data containing many rapid transitions between conductance levels, as described previously for AMPARs[44]. Accordingly, a resolution of two filter rise times (2 × 111 μs) was imposed to detect and account for brief events while maintaining resolution of small conductances. Digitally filtered data were exported to Signal 5.0 (Cambridge Electronic Design) for time-course fitting analysis with SCAN[45]. The idealized records were then used to provide information on response amplitudes, which could be fit with Gaussian functions whose peaks reflect discrete conductance levels: $y = \Sigma_{i=1.n}(A_i/w_i \times \mathrm{sqrt}(\pi/2))) \times \exp(-2 \times ((x-xc_i)/w_i)^2$ where A = area, xc = center of the peak, and w = error associated with xc. From this analysis, the distribution and amplitude of single-channel events observed in patches containing a few channels (**Fig. 2f**) were similar to events measured at equilibrium in multichannel patches (**Supplementary Fig. 5**).

Molecular dynamics simulations. All crystal structures used in this manuscript were obtained from the Research Collaboratory for Structural Bioinformatics (RCSB) protein data bank. Two protein structures were used for building models for the MD simulations: an L-Glu–bound GluK2 LBD dimer (PDB 3G3F (resolution 1.38 Å (ref. 46)) and an L-Glu–bound GluK2 Y521C L783C LBD dimer (PDB 2I0C (resolution 2.25 Å (ref. 15)), which was used only for simulations concerning the double-cysteine mutant. Together with the crystallographically resolved water molecules, L-Glu ligands and ions were retained in the simulation setup, whereas two bound isopropyl alcohol molecules were deleted. In simulations of GluK2 without bound sodium ions (**Supplementary Fig. 4**), these were removed before system setup. The protein was solvated in water in a (90 Å) (ref. 43) box with the TIP3P water model[47], whereafter the system was neutralized and 150 mM NaCl was added. Mutations, except for Y521C L783C, were imposed manually before simulation setup, either by editing or deleting atoms in the PDB file or by using the mutate function of PyMOL (http://www.pymol.org/) and adjusting the side chain rotamer. For the double-cysteine mutant, the GluK2 double-cysteine (Y521C L783C) mutant structure was used. This structure had no ions bound, so the interface-bound ions from the wild-type structure were added, and rotamers for side chains surrounding the ion sites were optimized in PyMOL before solvation, neutralization and ionization as described above.

The MD simulations were performed in Gromacs 4.5 (ref. 48) with the OPLS all-atom force field[49,50]. The systems were first energy minimized until the maximum force on an atom was <100 kJ/mol/nm. After energy minimization, a 200-ns restrained simulation with position restraints on protein heavy atoms and on bound ions with a force constant of 1,000 kJ mol^{-1} nm^{-2} was performed in the NVT ensemble with a temperature of 300 K maintained by a Berendsen thermostat[51]. Periodic boundary conditions were used, and van der Waals interactions were cut off at 10 Å. Long-range electrostatics were accounted for by the Particle-Mesh Ewald method[52]. All bonds were treated as constraints with the LINCS algorithm, allowing a time step of 2 fs. Subsequently, 100 ns of production run were performed (only 30–50 ns for E524G). The NPT ensemble was used with the temperature retained at 300 K and the pressure at 1 bar by the Berendsen thermostat and barostat, respectively[51]. Two repeats for each

mutational variant were produced. Analyses were performed with VMD[53] and analysis tools of GROMACS[48].

Statistical methods. Results are expressed as mean ± s.e.m. Statistical analyses of sample means were performed with two-tailed Student's *t* tests. $P < 0.05$ was considered to be statistically significant.

43. Khiroug, S.S. *et al.* Dynamic visualization of membrane-inserted fraction of pHluorin-tagged channels using repetitive acidification technique. *BMC Neurosci.* **10**, 141 (2009).
44. Zhang, W., Cho, Y., Lolis, E. & Howe, J.R. Structural and single-channel results indicate that the rates of ligand binding domain closing and opening directly impact AMPA receptor gating. *J. Neurosci.* **28**, 932–943 (2008).
45. Colquhoun, D. & Sigworth, F.J. in *Single Channel Recording* (eds. Sakmann, B. & Neher, E.) 483–587 (Plenum Press, 1995).
46. Chaudhry, C., Weston, M.C., Schuck, P., Rosenmund, C. & Mayer, M.L. Stability of ligand-binding domain dimer assembly controls kainate receptor desensitization. *EMBO J.* **28**, 1518–1530 (2009).
47. Jorgensen, W.L., Chandrasekhar, J., Madura, J.D., Impey, R.W. & Klein, M.L. Comparison of simple potential functions for simulating liquid water. *J. Chem. Phys.* **79**, 926–935 (1983).
48. Hess, B., Kutzner, C., Van Der Spoel, D. & Lindahl, E. GROMACS 4: algorithms for highly efficient, load-balanced, and scalable molecular simulation. *J. Chem. Theory Comput.* **4**, 435–447 (2008).
49. Jorgensen, W.L., Maxwell, D.S. & Tirado-Rives, J. Development and testing of the OPLS all-atom force field on conformational energetics and properties of organic liquids. *J. Am. Chem. Soc.* **118**, 11225–11236 (1996).
50. Kaminski, G.A., Friesner, R.A., Tirado-Rives, J. & Jorgensen, W.L. Evaluation and reparametrization of the OPLS-AA force field for proteins via comparison with accurate quantum chemical calculations on peptides. *J. Phys. Chem. B* **105**, 6474–6487 (2001).
51. Berendsen, H.J.C., Postma, J.P.M., Van Gunsteren, W.F., Dinola, A. & Haak, J.R. Molecular dynamics with coupling to an external bath. *J. Chem. Phys.* **81**, 3684–3690 (1984).
52. Darden, T., York, D. & Pedersen, L. Particle mesh Ewald: an $N\cdot\log(N)$ method for Ewald sums in large systems. *J. Chem. Phys.* **98**, 10089–10092 (1993).
53. Humphrey, W., Dalke, A. & Schulten, K. VMD: visual molecular dynamics. *J. Mol. Graph.* **14**, 33–38 (1996).

doi:10.1038/nsmb.2654